Popular Summary for
"A New Way to Measure Cirrus Ice Water Content by Using Ice Raman Scatter with Raman Lidar"

Zhien Wang
Submitted to *Geophysical Research Letters*

High and cold cirrus clouds mainly contain irregular ice crystals, such as, columns, hexagonal plates, bullet rosettes, and dendrites, and have different impacts on the climate system than low-level clouds, such as stratus, stratocumulus, and cumulus. The radiative effects of cirrus clouds on the current and future climate depend strongly on cirrus cloud microphysical properties including ice water content (IWC) and ice crystal sizes, which are mostly an unknown aspect of cirrus clouds. Because of the natural complexity of cirrus clouds and their high locations, it is a challenging task to get them accurately by both remote sensing and in situ sampling. This study presents a new method to remotely sense cirrus microphysical properties by using ice Raman scatter with a Raman lidar. The intensity of Raman scattering is fundamentally proportional to the number of molecules involved. Therefore, ice Raman scattering signal provides a more direct way to measure IWC than other remote sensing methods. Case studies show that this method has the potential to provide essential information of cirrus microphysical properties to study cloud physical processes in cirrus clouds.

A New Way to Measure Cirrus Ice Water Content by Using Ice Raman Scatter with Raman Lidar

Zhien Wang[1,2], David N. Whiteman[2], Belay Demoz[2] and Igor Veselovskii[1,2]

[(1)]GEST Center, University of Maryland Baltimore County, Baltimore, MD 21250 USA, zhien@agnes.gsfc.nasa.gov

[(2)] Mesoscale Atmospheric Processes Branch, GSFC, Greenbelt, MD 20771,USA

Abstract

To improve our understanding of cirrus cloud radiative impact on the current and future climate, we need improved knowledge of cirrus cloud microphysical properties. However, long-term studies of cirrus clouds indicated that it is a challenging task to get them accurately by both remote sensing and in situ sampling. This study presents a new method to remotely sense cirrus microphysical properties by using ice Raman scatter with a Raman lidar. The intensity of Raman scattering is fundamentally proportional to the number of molecules involved. Therefore, ice Raman scattering signal provides a more direct way to measure ice water content. Case studies show that this method has the potential to provide essential information of cirrus microphysical properties to study cloud physical processes in cirrus clouds.

Introduction

Cirrus clouds affect the surface and top-of-atmosphere energy budgets and can produce large local variations in atmospheric heating by heating at cloud bottom and cooling at cloud top. The degree and extent of the so-called greenhouse-versus-albedo effects involving cirrus clouds will lead to significant atmospheric differential cooling and heating in the vertical as well as on horizontal scales (Liou, 1986) and is dependent on cirrus microphysical properties and their vertical distribution (Stephens et al., 1990). However, it is a challenging task to measure cirrus Ice Water Content (IWC) and particle size by remote sensing or in situ sampling. The main limitations for in situ sampling are the small sampling volume and the high cost of collecting long-term data over different regions. IWC estimated from in situ particle size probes has large uncertainties associated with different ice crystal shapes and densities (Heymsfield et al. 2002). There have been significant advances in ground-based remote sensing of cirrus clouds using the Department of Energy Atmospheric Radiation Measurement (ARM) program Cloud and Radiation Testbed (CART) site measurements (Matrosov et al.,1994; Mace et al. 1998; Wang and Sassen, 2002). Nevertheless, uncertainty in the retrieved IWC by using lidar, radar, and radiometer measurements might be very large under some situations because one has to make several critical assumptions about cirrus clouds such as the size distribution and density of ice crystals, which vary a lot in cirrus clouds. A remote sensing method that possesses a signal that is directly related to IWC would be more promise for IWC measurements and would also be a great asset in studying these sensitivities in other techniques for obtaining IWC. Here, we report on a new method to remotely measure IWC using Raman scattering from ice in cirrus clouds. First, we briefly describe our Raman lidar system. Then we present the method and measurements. Results from a lidar-radar algorithm are used to calibrate the ice Raman scatter based retrieval algorithm.

Where C is a constant and IWC is ice water content ($C\,IWC = c_A N_a$). To account for the possible influences of the particle morphology, the morphology factor M is introduced. M is a function of the orientation, the size and the shape of the ice crystals for a given laser frequency. In lidar measurements, the Raman signal is integrated over a large volume temporally and spatially; therefore, the sensitivity of Raman scatter to ice crystal orientation and shape is reduced. Furthermore, Raman scattering intensity is fundamentally proportional to the number of molecules in the probed volume. Several experimental studies indicated that the Raman scatter from droplets with size parameters (2π r/λ) larger than 60 is roughly proportional to the volume of droplets if averaged over a small parameter range. Therefore, we regard M as a constant for the first order approximation.

Based on above discussion, the lidar equation of ice Raman scatter can be expressed as

$$P_{ice}(R) = \frac{C_{ice} P_0\, IWC\, \sigma_{ice}(\upsilon_0, \upsilon_{ice}, T)}{R^2} \exp\left(-\int_0^R (\alpha(\upsilon_0, r) + \alpha(\upsilon_{ice}, r))dr\right), \tag{3}$$

where P_{ice} is return power at the ice Raman scatter frequency υ_{ice}, P_0 is transmitted laser power, and R is the range from lidar station. C_{ice} is a new constant including lidar system constant and constants of C and M in Eq. (2). $\alpha(\upsilon_0,\text{r})$ and $\alpha(\upsilon_{\text{ice}}, \text{r})$ represent atmospheric extinction coefficients including the scatter and absorption of molecules and particles at frequencies υ_0 and υ_{ice} and range r, respectively.

For the Raman scatter of nitrogen, we have

$$P_{N_2}(R) = \frac{C_{N_2} P_0\, N_{N_2}(R) \sigma_{N_2}(\upsilon_0, \upsilon_{N_2}, T)}{R^2} \exp\left(-\int_0^R (\alpha(\upsilon_0, r) + \alpha(\upsilon_{N_2}, r))dr\right), \tag{4}$$

where N_{N2} is the number density of nitrogen at range R and υ_{N2} is the Raman scatter frequency of nitrogen.

Combining Eqs. (3) and (4), we have

$$IWC = \frac{P_{ice}(R)}{P_{N_2}(R)} \frac{C_{N_2} N_{N_2}(R) \sigma_{N_2}(\upsilon_0, \upsilon_{N_2}, T)}{C_{ice} \sigma_{ice}(\upsilon_0, \upsilon_{ice}, T)} \exp\left(-\int_0^R (\alpha(\upsilon_{N_2}, r) - \alpha(\upsilon_{ice}, r))dr\right), \tag{5}$$

On the right side of this equation, $P_{ice}(R)/P_{N2}(R)$ is known from lidar measurements; ($C_{N2}N_{N2}(R)\ \sigma_{N2}(\upsilon_0,\ \upsilon_{N2},\ T)\ /(C_{ice}\ \sigma_{ice}(\upsilon_0,\ \upsilon_{ice},\ T))$ can be approximated as $K(T)\ \beta(R)$, where $K(T)$ is a new constant and $\beta(R)$ is backscattering coefficient of molecules; the exponential term represents the difference of atmospheric attenuation difference at the two Raman channels and can be estimated from the Raman lidar measurements and atmospheric temperature profile. K might slightly depend on temperature, but we neglect the temperature dependency in this study. At wavelengths of υ_{ice} and υ_{N2}, the attenuation difference due to clouds is negligible because of small wavelength dependency of attenuation for large particles comparing with wavelength. Based on these discussions, Eq.(5) can be expressed as:

$$IWC = \frac{P_{ice}(R)}{P_{N_2}(R)} K\beta(R) \exp\left(-\int_0^R (\alpha(\upsilon_{N_2}, r) - \alpha(\upsilon_{ice}, r))dr\right), \tag{6}$$

Therefore, we only need to know K to determine IWC from SRL measurements, and an approach to determine K is presented below.

With retrieved IWC and estimated extinction coefficient from Raman lidar measurements, general effective size (D_{ge}) can be estimated by using relationship of $\alpha = IWC\ (-2.93599*10^{-4}+2.54540/D_{ge})$ developed by Fu (1996). When K is known, we obtain IWC and D_{ge} profiles from SRL measurements.

Measurements

During the Atmospheric Infrared Sounder (AIRS) Water Vapor Experiment-Ground (AWEX-G) between 27 October and 16 November 2003, the SRL was sited at the ARM Southern Great Plains (SGP) CART site. An example of SRL signals (10-min average) measured on 12 November is presented in Figure 2. During this time, cirrus cloud was between 6 and 9 km above ground level, and optical depth estimated from elastic and nitrogen channels is ~1.2. A strong signal was measured in the liquid/solid Raman channel in the cirrus layer as indicated by strong backscatter signal and moderate attenuation in the N_2 channel. Compared with the other signals, the Raman scattering from water vapor and ice is weak, but, the signal-to-noise ratios of them are good for analysis with 10-minute average.

As discussed above, we need to know the value of K to estimate IWC. If we know Raman scattering cross-section of ice and nitrogen, the optical transmittance of receiving system, and other system constants, we can calculate K directly. We hope to pursue this work in the future. Here, however, we use an alternative method to determine K by comparing with IWC or ice water path (IWP) derived from a published lidar-radar algorithm (Wang and Sassen 2002). The lidar-radar algorithm uses cirrus extinction coefficient derived from Raman lidar measurements and radar reflectivity factor to estimate IWC and D_{ge}. In this algorithm, the accuracy of IWC or IWP mainly depends on the accuracy of extinction coefficient or optical depth. Between extinction coefficient and optical depth derived from Raman lidar measurements, Optical depth has better accuracy due to its lower susceptibility to multiple scattering effects (Whiteman et al., 2001). Therefore, IWP is better than IWC for the intercomparison to calculate the constant K.

The AWEX-G field campaign provided a chance to use this approach to estimate K, and an example is given in Fig. 3. Figures 3a and 3b present time-height display of lidar scattering ratio from SRL and radar reflectivity factor (Ze) from the millimeter cloud radar at the SGP CART Site. To provide cirrus extinction coefficients for the lidar-radar algorithm, we simply multiply cirrus backscattering coefficients with a layer mean extinction-to-backscattering ratio estimated from optical depth and layer-integrated backscattering coefficient (Whiteman et al., 2001). IWC profiles retrieved from the lidar-radar algorithm are given in Fig. 3c. As mentioned above, We use IWP from the lidar-radar algorithm to determine K, and a comparison of IWP time series from the lidar-radar algorithm and from ice Raman signal is given in the Fig. 3e, which indicates that they agree well and follow the same pattern of variation. IWC profiles from ice Raman signal

are presented in Fig. 3d. Comparing Figs. 3c and 3e, we see good agreement between the two approaches. However, there are some differences between them, which may be caused by the uncertainties in the lidar-radar retrieval and the lower signal-to-noise ratio of Raman signal at some altitudes.

To examine the potential variation of K due to temperature and other factors, we perform the same calibration procedure on five different cirrus events during the AWEX-G. The results are listed in Table 1. These cases cover a mid-cloud temperature range of –24 to –60 degree with optical depth ranging from 0.05 to 2. The K calculated from each individual event range from 1.813 to 3.284. Comparing with the other days, the K on 2 November 2003 has relatively low value. This is an optically thin cirrus cloud with low Ze, and there are potential larger errors in K because of the relatively low signal-to-noise ice Raman signal and relative large percentage errors in estimated optical depth and measured Ze. Excluding this case, K has a mean of 2.875 with a standard deviation of 0.339, which is ~ 11.8% of the mean. Considering uncertainties in the IWP estimated from the lidar-radar algorithm, the variation range of K is reasonable and might mainly be caused by these uncertainties. Therefore, we use the mean for K to calculate IWC.

Applying the mean K to all cases, we can get IWC and Dge profiles. Comparisons of between IWP derived by the lidar-radar algorithm and that from ice Raman scattering are given in Fig. 4. In general, there are good agreements between these two methods. The intensity of Raman scattering is fundamentally proportional to the number of molecules involved, though the shape of the spectrum is slightly depend on temperature (Whiteman 2003). The change of the transmitted ice Raman intensity within 40 degree is expected to be less than 5 %. Therefore, it is reasonable to assume that K is the same during the AWEX-G because of the same optical configuration. Then, the periods when the two IWPs do not follow each other well might indicate potential errors in the lidar-radar method because of possible failures of assumptions in the algorithm or errors in the inputs. This figure shows a potential to use Raman IWC measurements to refine other remote sensing methods (Matrosov et al.,1994; Mace et al. 1998; Wang and Sassen, 2002).

Conclusions

This paper presented a new approach to remotely sense IWC and D_{ge} using the ice Raman signal observed by a Raman lidar. As demonstrated in the case studies, this method provides the essential information of cirrus microphysical properties to study cloud physical processes in cirrus clouds. The main limitation of this method is weak ice Raman signal. But, the signal presented in this paper can be improved a lot. First, it can be improved by optimal design of the filter to include main ice Raman scattering spectrum. In the current SRL, the filter was optimized for liquid water measurements. Second, it can be improved by increasing transmitted laser power. The laser power for measurements presented in this paper is only about 7 W. With improvements such as these, increases in signal to noise of between 2-4 can be expected. Therefore, Raman lidar might be an effective tool to measure IWC and D_{ge} for cirrus cloud study during nighttime. A Raman lidar operated from an aircraft, such as the NASA/GSFC Raman

Airborne Spectroscopic Liar (RASL at http://ramanlidar.gsfc.nasa.gov), might provide an effective alternative method for in situ IWC measurements with much large sampling volume than other approaches. Moreover, this method might provide measurements to refine other techniques for IWC measurements.

Acknowledgements. This research has been partly supported by NASA and DOE grant DE-FG02-03ER63536 from the Atmospheric Radiation Measurement Program. We thank Dr. Bunkin at General Physics Institute, Russian Academy of Sciences for providing us Raman spectra data of ice and water.

Reference:

Bunkin, A. F., G. A. Lyakhov, N. V. Suyazov, and S. M. Pershin (2000), Sequence of water thermodynamic singularities in Raman spectra, *J. Raman Spectrosc., 31*, 857-861.

Fu, Q. (1996), An accurate parameterization of the solar radiative properties of cirrus clouds for climate models, *J. Climate, 9*, 2058-2082.

Heymsfield, A. J., S. Lewis, A. Bansemer, J. Iaquinta, L. M. Miloshevich, M. Kajikawa, C. Twohy, and M. R. Poellot (2002), A general approach for deriving the properties of cirrus and stratiform ice cloud particles, *J. Atmos. Sci., 59*, 3-29.

Liou, K. N., 1986, Influence of cirrus clouds on weather and climate processes: A global perspective, *Mon. Wea. Rev., **114***, 1167-1199.

Loudon, R. (2001), The Raman effect in crystals, *Advances in Physics, 50*, 813-864.

Mace, G. G., T. A. Ackerman, P. Minnis, and D. F. Young (1998), Cirrus layer microphysical properties derived from surface-based millimeter radar and infrared interferometer data, *J. Geophys. Res., 104*, 16741-16753.

Matrosov, S. Y., B. W. Orr, R. A. Kropfli, and J. B. Snider (1994), Retrieval of vertical profiles of cirrus cloud microphysical parameters from Doppler radar and infrared radiometer measurements. *J. Appl. Meteor.,33*, 617-626.

Scherer, J.R. and R. G. Snyder (1977), Raman intensity of single crystal ice I_h, *J. Chem. Phys., 67*, 4794-4811.

Stephens, G. L., S. C. Tsay, P. W. Stackhouse, and P. J. Flatau (1990), The relevance of rhe microphysical and radiative properties of cirrus clouds to climate and climatic feedback, *J. Atmos. Sci., 47*, 1742-1753.

Tobin, M. C. (1971), Laser Raman Spectroscopy. In Chemical Analysis, edited by P. J., Elving and I. M. Kolthoff, Wiley, New York.

Vehring, R., C. L. Aardahl, G. Schweiger, and E. J. Davis (1998), The characterization of fine particles originating from an uncharged aerosol: Size dependence and detection limits for Raman analysis, *J. Aerosol Sci., 29*, 1045-1061.

Venkatesh, C. G., S. A. Rice, and J. B. Bates (1975), A Raman spectral study of amorphous solid water, *J. Chem. Phys., 63*, 1065-1071.

Wang, Z. and K. Sassen (2002), Cirrus cloud microphysical property retrieval using lidar and radar measurements: I algorithm description and comparison with in situ data, *J. Appl. Meteor., 41*, 218-229.

Whiteman, D. N., K. D. Evans, B. Demoz, D. O'C Starr, E. W. Eloranta, D. Tobin, W. Feltz, G. J. Jedlovec, S. I. Gutman, G. K. Schwemmer, M. Cadirola, S. H. Melfi, and

Figure Caption:

Figure 1: Water and ice Raman scatter spectrum and the transmission of solid/liquid and water vapor filters used in SRL.

Figure 2: An example of SRL signals (10-min average) measured on 12 November 2003 at the SGP CART site.

Figure 3: Time-height display of lidar scattering ratio (a), radar reflectivity factor (Ze, b), IWC from the lidar-radar algorithm(c), IWC using ice Raman signal (d), and the intercomparison of IWP derived from these two methods (e) observed at the SGP CART Site on 31 October 2003.

Figure 4: Comparisons of IWPs derived by the lidar-radar algorithm and from ice Raman scatter using a mean K for the five cirrus cloud cases summarized in the Table 1.

Table 1: The statistics of cirrus macrophysical properties and the K for the five cirrus events during the AWEX.

Date	10/30/2003	10/31/2003	11/2/2003	11/4/2003	11/12/2003
Mean Cloud Base Height (km)	10.5	11.0	11.4	10.2	6.0
Mean Cloud Top Height (km)	12.0	13.8	12.2	12.5	9.1
Mean Middle cloud temperature (°C)	-52.4	-59.2	-51.5	-48.5	-23.8
Mean Optical Depth	0.356	0.736	0.155	0.899	1.225
K	2.975	2.483	1.813	2.756	3.284
IWP correlation coefficient	0.986	0.964	0.950	0.886	0.974

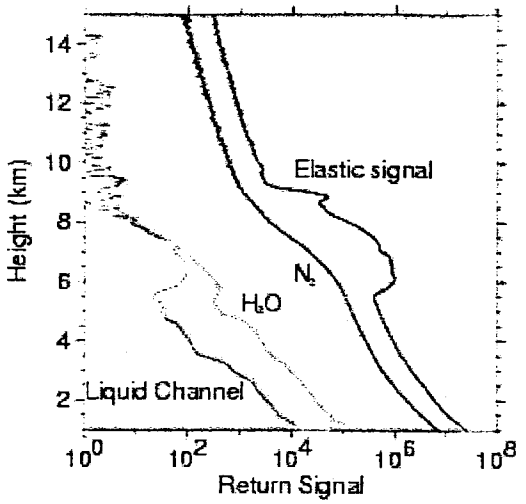
Height (km)
14
12
10
8
6
4
2
Elastic signal
N2
H2O
Liquid Channel
10^0
10^2
10^4
10^6
10^8
Return Signal

Fig. 2

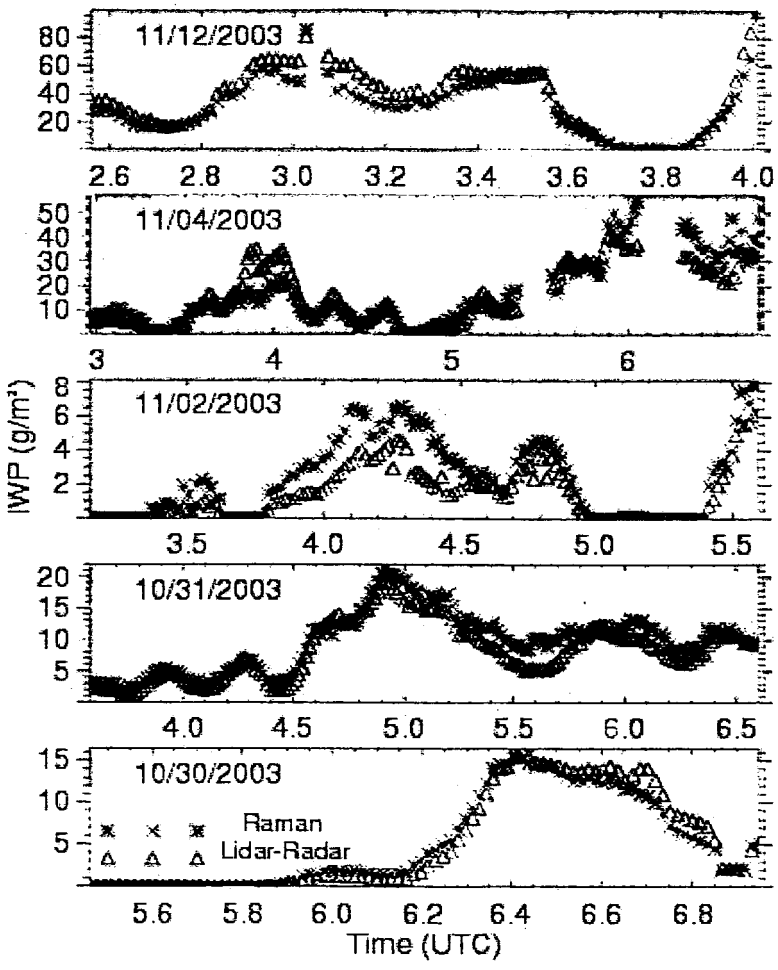
11/12/2003
11/04/2003
11/02/2003
10/31/2003
10/30/2003
Raman
Lidar-Radar
IWP (g/m²)
Time (UTC)

Fig. 4

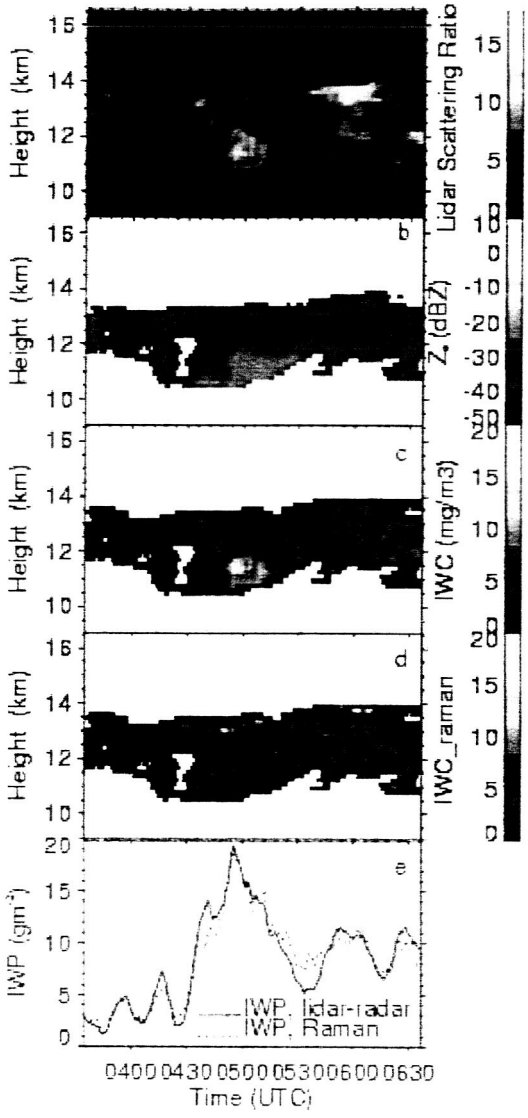
Height (km)
15
14
12
10
b
c
d
Lidar Scattering Ratio
Z_e (dBZ)
IWC (mg/m3)
IWC_raman
IWP (gm-2)
e
IWP, lidar-radar
IWP, Raman
0400 0430 0500 0530 0600 0630
Time (UTC)

Fig. 3

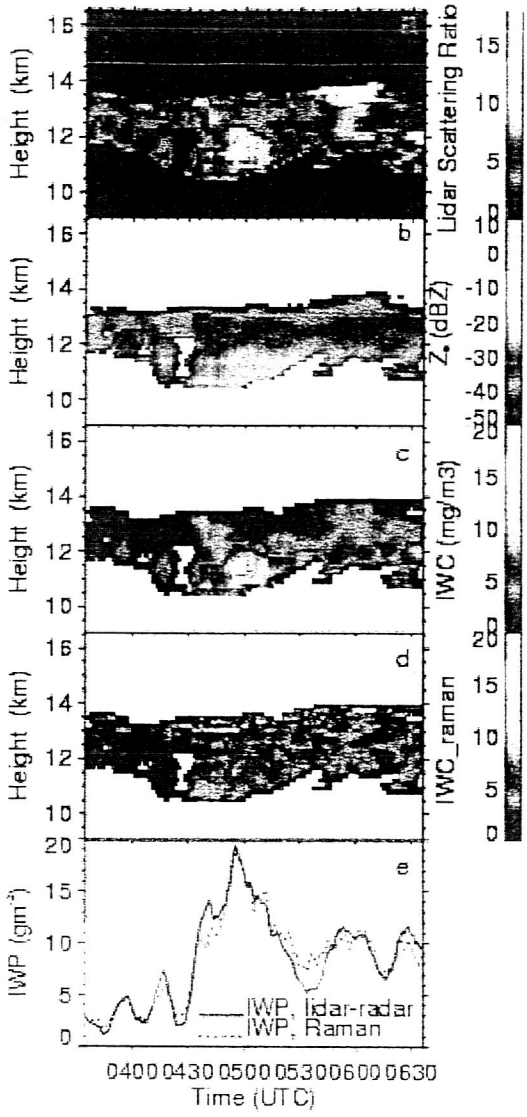
Height (km)
Lidar Scattering Ratio
b
Z (dBZ)
c
IWC (mg/m3)
d
IWC_raman
e
IWP (gm-2)
IWP, lidar-radar
IWP, Raman
0400 0430 0500 0530 0600 0630
Time (UTC)

Fig. 3